Paper No. 251—32

Development of Plastic Gears for Power Transmission*

(Abnormal Wear near Tooth Root and Tooth Fracture near Pitch Point)

By Kenichi TERASHIMA**, Naohisa TSUKAMOTO***, Noriteru NISHIDA+, and Jiasun SHI++

Plastic gears have many excellent characteristics which are lacking in metallic gears, such as corrosion resistance, self-lubrication, quiet running, and so forth. The meshing behavior of plastic gears is very different from that of metallic gears. Therefore, the life estimation is very difficult for plastic gears. In this paper, generating and growing mechanisms of abnormal wear which appears fatally near the root of plastic tooth are analyzed, and then it is clarified that tooth fractures which take place frequently near pitch point are caused by abnormal wear. Additionally, some methods for extending the life of plastic gears are proposed.

Key Words : Gear, Plastic gear, Nylon gear, Deflection, Wear, Load sharing coefficient, Temperature, Crack, Fracture

1. Introduction

Plastic gears have many excellent properties, which are lacking in metallic gears, such as corrosion resistance, self-lubrication and silent running. However, for power transmission, they have some weak points such as insufficient load capacity and lower surface durability. Moreover, their mechanical strength decreases with a rise of tooth temperature, so it is difficult to estimate their lives.

In the previous report[1], the power transmitting mechanism of plastic gears was analyzed.

In this report, the following two mechanisms are clarified. One is the growing mechanism of abnormal wear near the root of plastic gear teeth and the other is that of a crack which appears near the pitch point and influences the life of plastic gears.

Table 1 defines symbols and subscripts used in this paper and gives specifications of test gears and running conditions.

2. Wear of Plastic Gears

2.1 Real state of wear

As the plastic is easily worn, the deterioration of tooth profile by wear becomes a problem. Figure 1 shows the growing process of wear of plastic teeth in a gear pair with m=5, Z_p=17 and Z_s=37. This gear pair was rotated at a load of p_n=49 N/mm and a pinion speed of n_p=20 rev s^{-1}. The amount of wear in Fig.1 includes the quantity of the permanent deformation of working tooth flank as shown in Fig.2. The important matter known from these figures is that at an early stage of operation (N_T5×10⁴, 42 min), wear with a depth of 60 μm occurs at the dedendum flank and rather deep wear appears at the pitch point where less wear is expected.

The wear quantity dw of the tooth flank may be assumed to be proportional to the frictional work $\mu\beta p_n(v_p-v_s)dt$, where v_p-v_s is the relative sliding velocity. So, the wear depth ds can be written as follows.

Table 1 Specification and running condition

Suffixes p,s or $1,2$ } Plastic gear, Steel gear
Abbreviations P-gear, S-gear }
Position marks t:Tip, w:Worst loading point
p:Pitch point, i:Inner worst point
f:Fillet

Item	Symbol	Specification
Module	m	5
Pressure angle	α_c	20°
Number of teeth	Z_p, Z_1	17
	Z_s, Z_2	37
Face width	b	10 mm
RPM of gear	n_p	20 s^{-1}
Normal load	p_n	49 N/mm
Material	MC-nylon*	(Hobbed)
(Machining)	S45C	(Shaved)
Total no. of rev.	N_T	
Specific sliding	σ_p	
Load sharing ratio	β	
Lubrication		Dry

* Improved 6-nylon

* Received 25th June, 1983.
** Professor, Huazhong University of Science and Technology, Wuhan, Hubei, P.R.CHINA
*** A.Professor, Chiba Institute of Technology, Narashino City, JAPAN
+ A.Professor, Faculty of Engineering, Nagasaki University, Nagasaki, JAPAN
++ Manager, Baoji Fork Lift Manufactory, Baoji City, P.R.CHINA

$$ds=K_1\mu\beta p_n(v_p-v_s)/(v_p\rho_p),$$

where K_1 is a proportional constant and ρ_p is the density of plastic. In the above equation, K_1, ρ_p, μ and p_n are constants. Therefore, we get

$$ds=c_p\beta\sigma_p \quad \cdots\cdots (1)$$

where the constant $c_p=K_1\mu p_n/\rho_p$ and the specific sliding $\sigma_p=(v_p-v_s)/v_p$.

From Fig.3, the sliding velocities v_p, v_s and the specific sliding σ_p at the meshing point Q at a distance l from the pitch point p, are written as follows.

$$\left.\begin{aligned} &l_1=\sqrt{r_{o1}^2-r_{g1}^2},\quad l_2=\sqrt{r_{o2}^2-r_{g2}^2}\\ &\alpha_1=\tan^{-1}\{(l_1-l)/r_{g1}\}\\ &\alpha_2=\tan^{-1}\{(l_2+l)/r_{g2}\}\\ &r_1=r_{g1}/\cos\alpha_1,\quad r_2=r_{g2}/\cos\alpha_2\\ &\omega_1=2\pi n_p/60,\quad \omega_2=\omega_1 Z_p/Z_s\\ &v_p=r_1\omega_1\sin\alpha_1,\quad v_s=r_2\omega_2\sin\alpha_2\\ &\sigma_p=(v_p-v_s)/v_p,\ \sigma_s=(v_s-v_p)/v_s \end{aligned}\right\} \quad \cdots\cdots (2)$$

When two pairs of teeth mesh at the worst loading point w and the root point f as shown in Fig.4, assuming that the wear depths of tooth flanks at these two points are g_w, g_f and their difference $g=g_f-g_w$ and tooth deflections at the above points are δ_w and δ_f respectively, the load sharing ratios β_w and β_f are described as follows.

$$\left.\begin{aligned} &\beta_f+\beta_w=1,\ \beta_f\delta_f+g=\beta_w\delta_w\\ &\therefore\quad \beta_f=(\delta_w-g)/(\delta_f+\delta_w) \end{aligned}\right\}$$

similarly, load sharing ratios β_i and β_t at the points i and t respectively can be obtained by introducing $g=g_i-g_t$, as follows.

$$\left.\begin{aligned} &\beta_i=(\delta_t-g)/(\delta_i+\delta_t),\quad \beta_t=1-\beta_i \end{aligned}\right\} \quad \cdots\cdots (3)$$

In Fig.5(a), the growing process of the wear shown in Fig.1 is drawn on the tooth profile. Figure 5(b) shows an example of specific sliding σ_p calculated by Eq.(2). Figure 5(c) shows the value of β at $g=0$ in

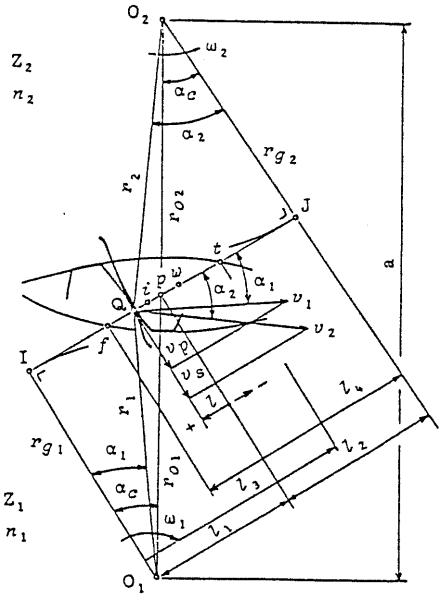

Fig.3 Sliding velocity and specific sliding

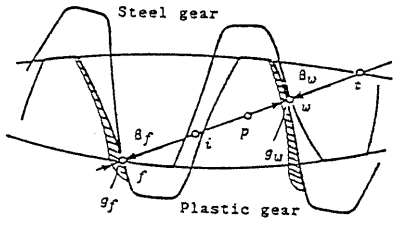

Fig.4 Load sharing ratio for worn teeth

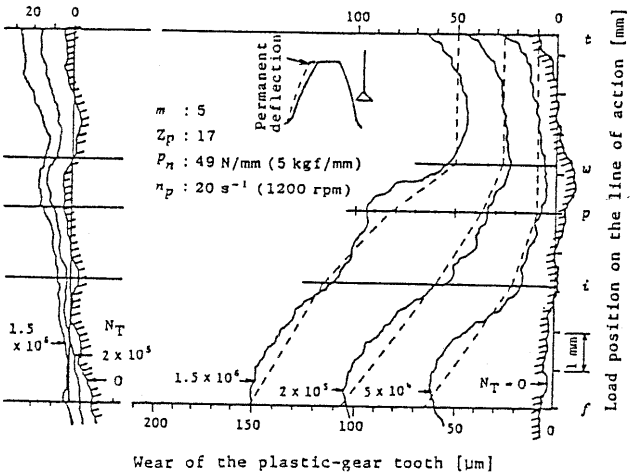

Fig.2 Permanent deflection

Fig.1 Growing process of wear

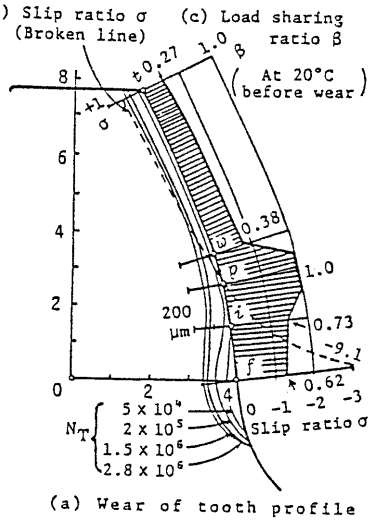

Fig.5 Wear, specific sliding and load sharing ratio

Eq.(3). The abnormal wear of tooth flank grows rapidly between the inner worst point i and the root point f. Thereafter, it spreads to the pitch point p and then reaches the outer worst point w. Normal wear occurs on the surface between the point w and the tip point t. This growing process of wear is a common tendency in plastic gears.

From Fig.5, it can be understood that severe wear appears near the root where the specific sliding is large. However, it can not be explained by the theory of the wear depth denoted by Eq.(1) why severe wear of the root grows rapidly in the short time of operation and why the groove wear occurs along pitch line where the specific sliding is zero.

2.2 Generation of wear and its growing mechanism

The reason for abnormal wear which grows rapidly near the tooth root in the short time of operation can be explained as follows. At a point L (shown in Fig.6) in one pair meshing region, the tooth deflection of plastic gears is large because the load sharing ratio β is unity. Therefore, the rotation of the driven steel gear delays and the corner S of the tooth tip of steel gears goes into the root of plastic teeth with gear rotation.

In Fig.6, under no load, two tooth flanks contact at the point L with distance l from w on the line of action. Under a certain load, the plastic tooth deflects by δ on the line of action and consequently, the contact point of tooth flanks moves to the point L'. The deflection δ can be calculated by Eq.(5). In this instance, the rotation of steel gear delays by δ.

We introduced two tangentials ($\overline{TS}$ and $\overline{SN}$) to the base circles from the point S on the tip circle of the driven gear. The following relations can be obtained:

$$\zeta=\cos^{-1}(R_{g2}/R_{k2})-\alpha_c+(l+\delta)/R_{g2}$$
$$x=R_{k2}\sin\zeta,\ y=R_{k2}\cos\zeta$$
$$R_s=SO_1=\sqrt{x^2+(a-y)^2},\quad l_4=\sqrt{R_{k2}^2-R_{g2}^2}$$
$$\xi=\angle SO_1O_2=\tan^{-1}\{x/(a-y)\}$$
$$\omega=\angle IO_1T=\cos^{-1}(R_{g1}/R_s)+\xi-\alpha_c$$
$$ST=\sqrt{R_s^2+R_{g1}^2}$$
$$UT=a\sin\alpha_c-l_4-l+R_{g1}\omega$$
$$\Delta S=ST-UT$$

For $\Delta S<0$, engraving occurs.

When the coordinate of point S is represented by the XY coordinate fixed on the following plastic tooth, we get

$$IM=a\sin\alpha_c-l_4-l$$
$$R_m=O_1M=\sqrt{R_{g1}^2+IM^2}$$
$$\phi_m=\angle MO_1Y=0.5\pi/Z_p+inv\alpha_c-inv\cos^{-1}(R_{g1}/R_m)$$
$$\phi_s=\angle SO_1Y=\phi_m+\alpha_c-\tan^{-1}(IM/R_{g1})-\xi$$
$$X=R_s\sin\phi_s,\ Y=R_s\cos\phi_s$$

.....(4)

Figure 7 shows the values of tooth deflections δ_i, δ_p and δ_w under unit load at the points i, p and w respectively. These points are in the one pair meshing region. These deflections can be calculated by the method shown in the previous report[1]. The deflection δ can be calculated from the following equations.

$$\left.\begin{aligned}&\delta=\bar{a}l^2+\bar{b}l+\delta_w\\&\bar{a}=\frac{(\delta_i-\delta_w)\,\overline{pw}-(\delta_p-\delta_w)\,\overline{iw}}{\overline{pw}\ \overline{iw}\ (\overline{iw}-\overline{pw})}\\&\bar{b}=(\delta_p-\bar{a}\,\overline{pw}^2-\delta_w)/\overline{pw}\end{aligned}\right\}\quad\text{.....(5)}$$

The distances between the points f, i, p, w and t shown in Eq.(5) and Fig.7 are obtained from Fig.6 as follows.

$$l_3=lt=\sqrt{R_{k1}^2-R_{g1}^2},\quad t_n=\pi m\cos\alpha_c$$
$$\overline{ft}=l_3+l_4-a\sin\alpha_c,\quad \overline{fi}=\overline{wt}=\overline{ft}-t_n$$
$$\overline{ip}=l_4-l_2-\overline{fi},\quad \overline{pw}=l_3-l_1-\overline{wt}$$
$$\overline{iw}=\overline{ip}+\overline{pw}$$

.....(6)

The values of δ_i, δ_p and δ_w at temperatures of 20 and 50°C can be obtained by the method mentioned in the previous report[1]. By substituting these values into Eqs.(6)

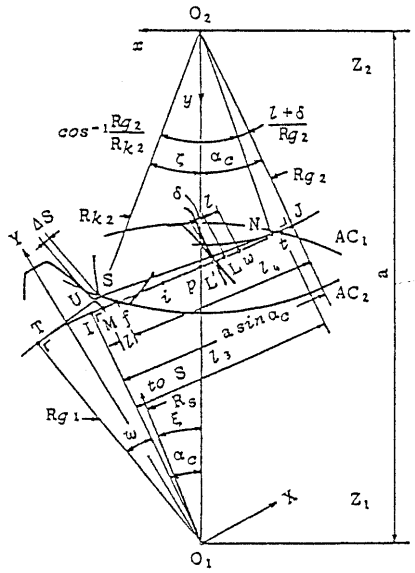

Fig.6 Interference near tooth root

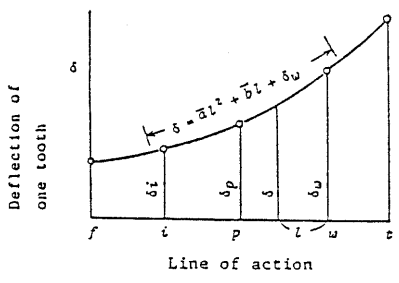

Fig.7 Deflection near pitch point

and (5), $\bar{a}$ and $\bar{b}$ can be obtained. When the value of l is increased gradually from zero, the locus of corner S is obtained from Eq.(4) as shown in Fig.8.

The corner S contacts with the plastic tooth flank at the point g when the temperature is 20°C, and at the point a when 50°C. And then it scrapes the tooth flank gbf at 20°C and deeply goes into the flank along the curve acS at 50°C. The reason that the tooth root wears rapidly and deeply at the beginning of the operation can be understood from these facts. After the wear reaches a certain depth, the corner a, which is the intersection of the plastic tooth flank and the groove made by the steel tooth flank ce, is pressed like a supporting point of a lever and rubbed powerfully because the steel tooth draws a trochoid in the tooth space of plastic gear. The specific sliding in this area is about 15 times as much as that at the tooth tip. From the above mentioned, it can be understood that the wear grows rapidly in the region ΔaSd and the temperature of this area becomes higher than that of other region.

Figure 10(a) shows the growing process of abnormal wear, in which normal wear between points w and t in Fig.1 has been subtracted. From Fig.10(a), it can be known that the part ij is scraped by the corner of the steel tooth tip, and then the crest near the point i is rubbed. Finally the crest near the point p is rubbed and the wear spreads toward the tooth tip with increasing depth of the groove.

3. Mechanisms of Tooth Fractures

3.1 Actual state of fractures

Plastic gears have been designed in the same manner as in steel gears under the idea that the maximum bending stress is generated at the tooth fillet. However, the fracture at the tooth fillet is hardly seen in plastic gears except in low speed and heavy load operations. Under the running conditions shown in Table 1, a small crack is generated between the points p and w in the middle part of face width as shown in Fig.9(a). With an increase in running time, this crack propagates along the tooth trace with an increasing depth and finally reaches the tooth ends [Fig.9(b)]. The propagation of the crack is slow and rather long running time can be expected from the initiation of a crack to a tooth fracture. Most of cracks appear in the band-like zone between the points w and i shown in Fig.9(c).

3.2 Mechanisms of crack generation

It is estimated that a plastic tooth fracture takes place such that a larger load acts on the addendum flank on account of the abnormal wear and the plastic gear material in the middle part of the tooth profile becomes soft due to a temperature rise caused by rubbing. Figure 10(b) shows the load sharing ratio β calculated from Eq.(3) under assumption that the wear depth is equal to 100 μm and N_T= 2×10⁵ rev. From Fig.10(b), it can be known that at the beginning of operation the load is not transmitted near the tooth root because of the abnormal wear, but with the tooth being warmed and becoming soft, the load comes to be shared by the root and consequently the load acting on the addendum flank decreases.

To know the tooth temperature, three kinds of thermo-paints, which change their colors at 40, 50 and 60°C, were applied on the tooth end face. Figure 11 shows changes in temperature with running time on the tooth end surfaces when the test gears are rotated at a room temperature of 20 °C.

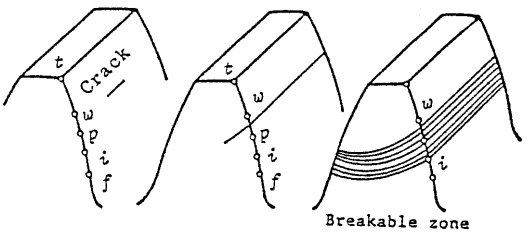

(a) Generation (b) Growth (c) Breakable zone

Fig.9 Crack generation and its growth

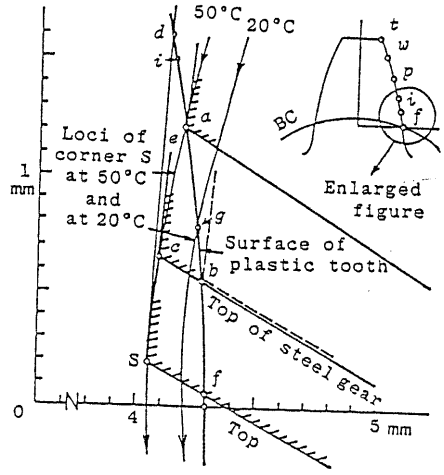

Fig.8 Scraping by tip corner of steel tooth

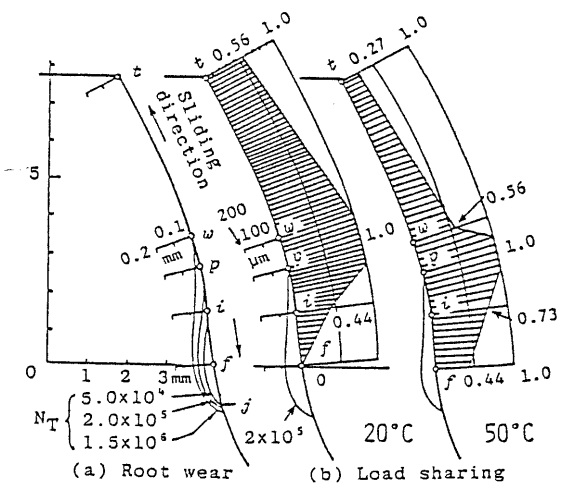

Fig.10 Abnormal wear near tooth root

Figure 11(a) shows isothermal lines on a plastic gear without wear. The highest temperature appears at first at the inner worst point i. With running time, the temperature rises as shown in the right hand sketches and the highest temperature is reached at 60°C. The part with the highest temperature corresponds to the point g in Fig.8. So, the temperature rise may be mainly caused by the heat caused by scraping.

Figure 11(b) shows that the high temperature part moves to near the pitch point p with growth of wear and the tooth temperature becomes lower than that in Fig.11(a). In this case, the wear depth g_f is 100 μm and the wear reaches the point p [Fig.1 and Fig.10(a)]. Because of this wear, the pitch point, at which the rolling contact is performed theoretically, is rubbed and pressed against the steel tooth surface designed to mesh with the plastic tooth at the point f near the root.

In Fig.11(c), the wear has grown enough and reached the point w (Fig.1). This point is rubbed and pressed powerfully and consequently a high temperature appears at this point. A remarkable point in these results is that the generation of heat becomes smaller after the abnormal wear has grown to some degree. This is because the tooth profile of plastic gears is changed by the wear and the deflection occurs so as to transmit the load smoothly.

As the heat generated in plastic gears contains not only the frictional heat between tooth surfaces but also the heat caused by the hysteresis loss in the viscoelastic material, it is very difficult to calculate the amount of the generated heat or the distribution of temperatures. We use Takanashi-Shoji's equation[2] to calculate the generated heat in the plastic gears with wear. From this equation, Eq.(7), the remainder of the generated heat in the plastic tooth can be obtained as shown in Fig.12(a). In Eq.(7), H_c [J] denotes the heat caused by the hysteresis loss, which is calculated on the assumption that the plastic tooth deflection can be expressed by Voigt models for viscoelastic bodies, and H_F [J] shows the remainder in the plastic gear of the frictional heat between tooth surfaces. The heat generated in one tooth during meshing of one pair of teeth is equal to $H_c + H_F$.

$$\left.\begin{aligned} H_c &= \frac{1}{10.2}\frac{t}{t_1}\frac{\beta^2}{2}\frac{p_n^2}{S}\left(1-e^{-\frac{2S}{\eta_D}t_1}\right) \\ H_F &= \frac{1}{10.2}\mu\beta p_n|v_p - v_s|\alpha_p \\ \alpha_p &= \frac{\sqrt{\lambda_p\rho_p C_p v_p}}{\sqrt{\lambda_p\rho_p C_p v_p}+\sqrt{\lambda_s\rho_s C_s v_s}} \end{aligned}\right\} \quad \cdots\cdots(7)$$

The symbols in Eq.(7) and their values

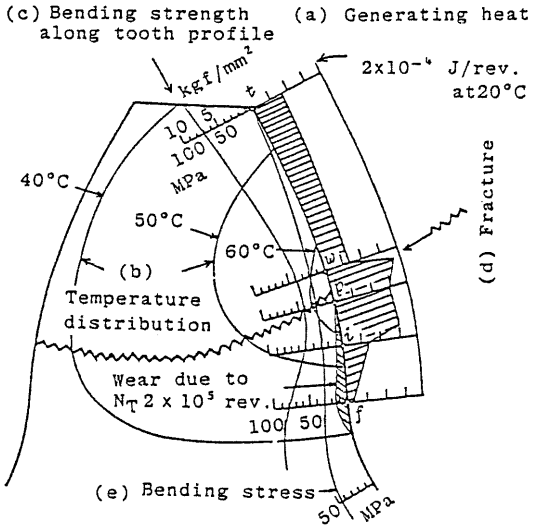

Fig.12 Generated heat, temperature distribution, tensile strength and bending stress

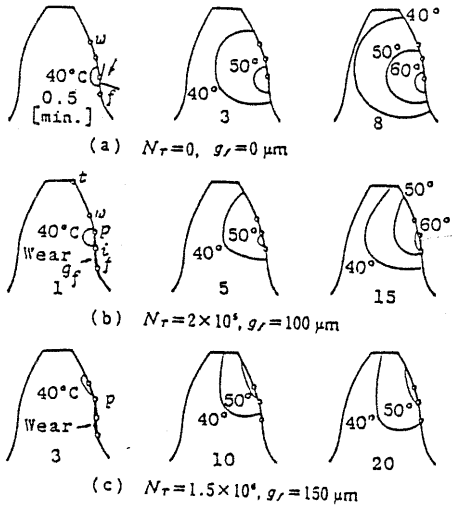

Fig.11 Wear, heat source and temperature distribution

Table 2 Values for calculation

Item	Symbol	Unit	Used value
Load sharing ratio	β		0.27 ∿ 1.00
Specific heat	c_p	J/kg K	1.92 x 10³
	c_s		0.47 x 10³
Dashpot viscosity	η_D	Ns/m	1177 ∿ 4119
Thermal conductivity	λ_p	W/m K	0.245
	λ_s		41.9
Kinematic friction coeff.	μ		0 ∿ 0.19
Specific weight	ρ_p	kg/m³	1.14 x 10³
	ρ_s		7.84 x 10³
Normal load	p_n	N/m	4.9 x 10⁴
Sliding velocity	v_p	m/s	0.25 ∿ 3.23
	v_s		1.18 ∿ 2.55
Spring constant	S	N/m	1.16 x 10⁶ ∿ 5.81 x 10⁶
Meshing period	t	s	2 x 10⁻⁴
Minute period	t_1		2 x 10⁻⁴

used for the calculation are shown in Table 2. The result of the calculation agreed well with the temperature distribution shown in Fig.12(b). The temperature near the pitch point is high. One of the authors confirmed by setting a thermo-couple in the inner and middle parts of the plastic tooth that the inner temperature was about 10°C higher than that of the end face of the tooth[3]. Figure 13 shows the inner temperature distribution estimated considering that the periphery and the end face of the gear are cooled by the rotation of gears, and that the temperature in the middle part of the face width is high. Figure 12(c) shows the estimated tensile strength of the plastic gear material in the middle part of the face width (section XX' in Fig.13), which is obtained by considering the influence of the temperature on the strength (Fig.14[4]).

The tensile strength of the plastic gear material [Fig.12(c)] is weakest at the pitch point and its value is 47 MPa. The bending fatigue limit[5] can be considered to be about 30% of the static strength, i.e., 13.7 MPa. The broken lines in Fig.12(d) and Fig.13 are drawn by connecting the tops of the isothermal lines in the section XX'. As the crack appears at the right end of the broken line at first and it extends along this line, this line can be considered to indicate the weakest section for tooth-tip loading. Figure 12(e) shows the bending stress on the tooth surface at a load of p_n=49 N/mm on the tooth tip. From Fig.12(e), it can be known that a pulsating stress of 22.5 MPa is generated at the pitch point.

The bending stress near the pitch point (22.5 MPa) is greater than a fatigue limit of 13.7 MPa at the same point. From this examination, the generation of a fatigue crack at this point can be understood.

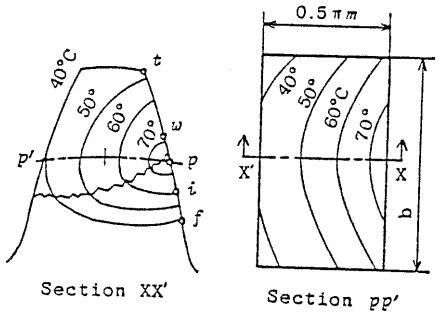

Fig.13 Estimated temperature distribution

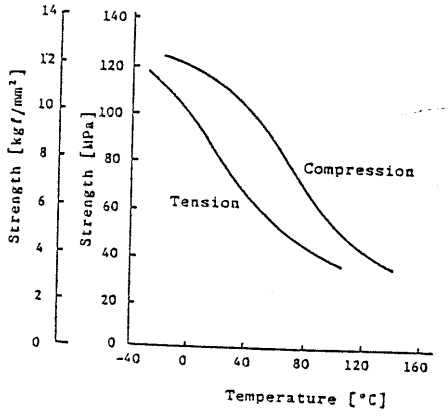

Fig.14 Strength of MC-nylon

4. Experiments to Confirm the Fracturing Mechanism and Methods to Increase Gear Life

4.1 Experiments to confirm the fracturing mechanism

From the aforementioned analyses, the process of the generation of a crack near the pitch point can be considered as follows. At first, abnormal wear is generated near the tooth root which results in severe rubbing near the pitch point. Owing to this, a higher temperature than the glass transition one appears and the gear material near the pitch point is softened and a crack is generated. In order to confirm this process, the life to fracture was examined by a test in which the gear was cooled continuously. The room temperature was kept at 18°C and a fan was used for cooling. Without cooling at the room temperature of 28°C, the tooth surface temperature at the pitch point was higher than 70°C and the total number of revolutions up to fracture, N_T, was 2.7×10^6 rev. But after cooling, the tooth surface temperature dropped below 50°C and the tooth did not fracture even after N_T= 6.6×10^7 rev. The life doubled when cooling was introduced.

4.2 Methods to extend the life

From the present theoretical analyses and experiments, the following can be considered effective to extend the life of plastic gears.

(1) As the wear increases in proportion to the total number of revolutions N_T (Fig.1), the plastic gear is better used as wheels which are subjected to a lower number of contacts than pinions.

(2) The temperature of tooth becomes high near the pitch point (Fig.12). Therefore, cooling of a gear pair is effective.

(3) The initial crack appears near the pitch point in the middle part of the face width [Fig.7(a)]. Application of slight caving to this part brings about retardation of the rise in temperature of this part due to a light contact with steel tooth surface[3].

(4) The tooth root of plastic gears is scraped by the corner of the tooth tip of steel gears, whether the gears are used as a driver or a follower. Therefore, tip relief or rounding of tip corners should be made with steel gears.

(5) The bending strength of plastics is about 1/7 that of steels and it decreases with a rise of temperature. So, it is desirable that the tooth thickness will be designed thick for plastic teeth and thin for steel teeth.

5. Conclusions

The generating and growing mechanisms of abnormal wear which appears near the root

of plastic gear tooth are clarified and the mechanism of crack initiation near the pitch point is revealed. The summary of this report is as follows.

(1) Abnormal wear near the root of plastic teeth is produced by scraping with the corner of the tooth tip of the mating steel gear, and the groove caused by the wear grows and extends to the outer worst point.

(2) The position where the generated heat becomes maximal is at the inner worst point while the scraping continues and it moves to the outer worst point through the pitch point with growth of the wear.

(3) It can be considered that the tooth temperature rise is most appreciable at a point between the inner worst point and the outer worst point, so the material becomes weaker at this point and a crack is generated and grown, finally a fracture taking place.

(4) To extend the life of plastic gears, the following can be considered to be effective. (i) Using them as wheel. (ii) Cooling the gear pair. (iii) Making a concave tooth trace error near the pitch point in the middle part of the face width. (iv) Adopting the tooth tip relief or rounding the corner of the crest of mating steel gear teeth.

References

(1) Terashima,K., Tsukamoto,N., and Jiasun, S., Development of Plastic Gears for Power Transmission, Bull. JSME, Vol.27, No.231(1984), p.2061.

(2) Takanashi,S. and Shoji,A., ASME Paper, No.80-C2/DET-107 (1980).

(3) Tsukamoto,N., Strength of Plastic Gears, Trans. Jpn. Soc. Mech. Eng. Vol.45, No. 391, C (1979), p.383.

(4) Nippon Polypenco Company, Technical Report of MC-nylon, (1984), p.3.

(5) Onoki,S., Mechanical Properties of Polymers and Composites, (1982), p.215, Kagakudoninsha.